

Graphical Abstract

Highlights

- A model based on a gamma distribution of diffusion coefficients for analysis of pulsed-field gradient NMR data is evaluated.
- The gamma model is substantially faster and easier to implement compared to the more wide-spread log-normal model.
- Results from experimental and simulated data show that the gamma model produces results very similar to those produced by the log-normal model.

(*) Corresponding author: Magnus Röding, Telephone: (+46) 31 772 49 92, E-mail: roding@chalmers.se, Address: Department of Mathematical Sciences, Chalmers University of Technology and Gothenburg University, 41296 Gothenburg, Sweden.

The gamma distribution model for pulsed-field gradient NMR studies of molecular-weight distributions of polymers

Magnus Röding(*)^a, Diana Bernin^b, Jenny Jonasson^a, Aila Särkkä^a, Daniel Topgaard^c, Mats Rudemo^a, Magnus Nydén^b

^a*Department of Mathematical Statistics, Chalmers University of Technology and Gothenburg University, Gothenburg, Sweden*

^b*Applied Surface Chemistry, Department of Chemical and Biological Engineering, Chalmers University of Technology, Gothenburg, Sweden*

^c*Division of Physical Chemistry, Center for Chemistry and Chemical Engineering, Lund University*

Abstract

Self-diffusion in polymer solutions studied with pulsed-field gradient nuclear magnetic resonance (PFG NMR) is typically based either on a single self-diffusion coefficient, or a log-normal distribution of self-diffusion coefficients, or in some cases mixtures of these. Experimental data on polyethylene glycol (PEG) solutions and simulations were used to compare a model based on a gamma distribution of self-diffusion coefficients to more established models such as the single exponential, the stretched exponential, and the log-normal distribution model with regard to performance and consistency. Even though the gamma distribution is very similar to the log-normal distribution, its NMR signal attenuation can be written in a closed form and therefore opens up for increased computational speed. Estimates of the mean self-diffusion coefficient, the spread, and the polydispersity index that were obtained using the gamma model were in excellent agreement with estimates obtained using the log-normal model. Furthermore, we demonstrate that the gamma distribution is by far superior to the log-normal, and comparable to the two other models, in terms of computational speed. This effect is particularly striking for multi-component signal attenuation. Additionally, the gamma distribution as well as the log-normal distribution incorporates explicitly a physically plausible model for polydispersity and spread, in contrast to the single exponential and the stretched exponential. Therefore, the gamma distribution model should be preferred in many experimental situations.

Keywords: Pulsed-field gradient NMR, self-diffusion, PEG, polymer, gamma distribution, log-normal distribution, molecular-weight distribution

1. Introduction

Pulsed-field gradient nuclear magnetic resonance (PFG NMR) is a powerful method to evaluate translational motion such as diffusion or flow [1, 2]. If the sample studied is sufficiently monodisperse, the (mean) self-diffusion coefficient can be obtained by fitting a single exponential function to the observed signal attenuation [3]. Also multi-component systems can easily be studied because of their chemical shift resolution. However, when the self-diffusion of for example a polymer is characterized by a molecular weight distribution and a corresponding distribution of self-diffusion coefficients, we obtain a more complex signal attenuation [4, 5, 6, 7]. The probability distribution of self-diffusion coefficients may be extracted by using an inverse Laplace transform, typically using the CONTIN framework, where no specific functional form or shape assumptions are imposed, but the solution is regularized for smoothness [8, 9, 10, 11]. Even though being notoriously difficult and very noise-sensitive, this approach has been widely applied in various techniques, e.g. NMR relaxation and diffusion measurements, and dynamic light scattering [12, 13]. An alternative approach is to assume a specific but flexible functional form, using e.g. the so-called stretched exponential, cumulant expansions, or a log-normal distribution model [14, 15, 5]. Many functional forms yield more or less identical fits and results in terms of the first two moments of a distribution (mean and variance) [16]. Thus, it is possible to choose the specific functional form based on simplicity and computational convenience.

In this paper, we propose to use a model based on a gamma distribution of self-diffusion coefficients. We discuss and compare different models for evaluating the NMR signal attenuation obtained from a PFG NMR experiment of polymers in water. In particular, we compare the computational speed and performance of the gamma model to the single exponential, the stretched exponential, and the log-normal models, all of which are already accepted and spread within the community. Although the gamma distribution has been mentioned in the literature as a model for a distribution of self-diffusion coefficients [15], its performance and suitability for the analysis of PFG NMR data appears not to have been thoroughly evaluated. To do this is the purpose of this work.

We first describe the basic theory and put the gamma distribution model in context. Then, we evaluate the single exponential, the stretched exponential, the log-normal, and the gamma model on experimental data sets of two polyethylene glycol (PEG) solutions with different polydispersity and also on several simulated data sets. The models are compared in terms of estimated mean self-diffusion coefficient, spread and polydispersity index. The performance of the gamma distribution model is compared to all other models, and in particular to its most obvious competitor, the log-normal distribution model.

2. Theory

For a single self-diffusion coefficient, Stejskal and Tanner [17] showed that the echo decay is exponential (the so called *single exponential model*),

$$I(k) = I_0 \exp(-k\langle D \rangle), \quad (1)$$

where I_0 is the signal intensity before decay (for $k = 0$), $\langle D \rangle$ is the mean self-diffusion coefficient (actually, it is the only one, but we stick to the $\langle D \rangle$ notation for consistency), and

$$k = (\gamma g \delta)^2 \left(\Delta - \frac{\delta}{3} \right). \quad (2)$$

Here, γ is the proton magnetogyric ratio ($\gamma = 2.6752 \times 10^8 \text{ rad T}^{-1}\text{s}^{-1}$), g is the gradient strength, δ is the gradient pulse duration, and Δ is the time lapse between the leading edges of the gradient pulses. In a plot of $\log I(k)$ vs k , a single self-diffusion coefficient will manifest itself by a linear decay (straight line). Generally, the echo attenuation shows non-linear behavior for molecules with a large degree of polydispersity. The obvious interpretation is that a single self-diffusion coefficient can not accurately describe the features of the system. Perhaps the simplest way of dealing with this problem is to use the *stretched exponential model*,

$$I(k) = I_0 \exp(-(kD_{\text{app}})^\beta), \quad (3)$$

a phenomenological relationship which is able to express polydispersity to some extent through the 'stretch' parameter β [18, 19], and some attempt have been made to interpret this in terms of polydispersity [20]. However, the relation between spread and the value of the beta parameter is complicated [20]. However, the stretched exponential model does not correspond to an actual *distribution* of self-diffusion coefficients. Accordingly, there is no expression relating D_{app} , the *apparent* self-diffusion coefficient, to the true, mean self-diffusion coefficient $\langle D \rangle$; however, as was pointed out by Callaghan (personal communication) it can be shown that

$$\left\langle \frac{1}{D} \right\rangle = \frac{\frac{1}{\beta} \Gamma\left(\frac{1}{\beta}\right)}{D_{\text{app}}}, \quad (4)$$

where Γ is the gamma function. However, since $\langle 1/D \rangle^{-1} \neq \langle D \rangle$, any estimate of the mean self-diffusion coefficient will be weighted toward the slowly diffusing molecules. Therefore, a more physically adequate approach is to start by assuming that the self-diffusion coefficient D follows a probability distribution $P(D)$, which yields that the attenuation is an integral (weighted sum) over different exponential decays,

$$I(k) = I_0 \int_0^\infty P(D) \exp(-kD) dD. \quad (5)$$

In general, the functional form of $P(D)$ is unknown [6]. However, a very common assumption is that the self-diffusion coefficients are log-normally distributed [21].

The log-normal distribution has probability density

$$P_L(D; \mu, \sigma_L) = \frac{1}{D\sqrt{2\pi\sigma_L^2}} \exp\left(-\frac{(\log D - \mu)^2}{2\sigma_L^2}\right), \quad (6)$$

with $\mu = \log(\langle D \rangle) - \sigma_L^2/2$ where $\langle D \rangle$ is the mean of D , and $\sigma_L^2 = \log(1+CV^2)$. The spread, or coefficient of variation (CV), is defined as $CV = (\text{standard deviation} / \text{mean}) \times 100\%$. However, the log-normal distribution does not yield an analytically tractable integral in Eq. (5). We suggest an alternative for the distribution $P(D)$ that does yield a tractable integral, namely the gamma distribution,

$$P_G(D; \kappa, \theta) = D^{\kappa-1} \frac{\exp(-D/\theta)}{\Gamma(\kappa)\theta^\kappa}, \quad (7)$$

where Γ is the gamma function, κ is the 'shape' parameter, and θ is the 'scale' parameter. Replacing $P(D)$ in Eq. (5) with P_G gives the echo decay model

$$I(k) = I_0(1 + k\theta)^{-\kappa}, \quad (8)$$

which can be written by using mean self-diffusion coefficient $\langle D \rangle$ and standard deviation σ_G as

$$I(k) = I_0(1 + k\sigma_G^2/\langle D \rangle)^{-\langle D \rangle^2/\sigma_G^2} \quad (9)$$

(see Appendix A for details regarding the gamma distribution model). This latter expression is not only more transparent to the practitioner, but was also found to be more numerically well-behaved. We will be interested in the spread CV and the polydispersity index, defined as

$$\text{PDI} = \frac{M_w}{M_n}, \quad (10)$$

where M_w and M_n are the weight-average and the number-average molecular weights, respectively [22]. The polydispersity index is per se a measure of the width of the *molecular-weight distribution*, whereas with PFG NMR we estimate the *self-diffusion coefficient distribution*. The self-diffusion coefficient D can be related to the molecular weight M by

$$D = KM^{-\alpha}, \quad (11)$$

with K and α being scaling parameters. From the parameters of the self-diffusion coefficient distribution, the polydispersity index can be computed as

$$\text{PDI} = \exp\left(\frac{\sigma_L^2}{\alpha^2}\right) \quad (12)$$

for the log-normal model and by

$$\text{PDI} = \left(1 + \frac{\sigma_G^2}{\langle D \rangle^2}\right)^{1/\alpha^2} \quad (13)$$

for the gamma model (see Appendix B for details about the polydispersity index calculations). In this paper we use $\alpha = 0.525$, the value previously measured for dilute PEG in water [6].

For multiple components which can not be resolved due to their chemical shift, it is assumed that the signal attenuation is a weighted sum of several attenuations of any of the above types.

Fitting the models to data is performed by the standard non-linear least squares method [23]. We minimize the sum

$$S = \sum_n (I_{\text{obs}}(k_n) - I(k_n))^2, \quad (14)$$

where $I_{\text{obs}}(k_n)$ is the normalized signal intensity for $k = k_n$, yielding least squares (or equivalently, if the noise truly is Gaussian and independent, maximum likelihood [24, 25]) estimates of the parameters for the chosen model.

3. Materials and methods

3.1. Materials

Two different polyethylene glycol (PEG) solutions were prepared using either a 11840 g mol⁻¹ PEG (Agilent Technologies, United Kingdom) or a 15000 g mol⁻¹ PEG (Sigma Aldrich, MO, United States), with different polydispersity index. PEG was dissolved in an appropriate amount of D₂O (99.8 %, Armar Chemicals, Switzerland) to achieve a concentration of 0.1% (w/w) ensuring independence of the parameter α of the different molecular weights in these distributions. Standard 5 mm NMR tubes were filled with 400 μ l. We denote the two PEG solutions by PEG I (PEG 11840) and PEG II (PEG 15000) for convenience.

3.2. Self-Diffusion Measurements

¹H PFG NMR experiments were carried out on a 600 MHz Bruker (Bruker, Germany) equipped with a diffusion probe (Diff30, providing a maximum gradient strength of 12 Tm⁻¹). A standard spin echo sequence was used with $\Delta = 100$ ms and a gradient pulse duration δ of 2 ms. Gradient strengths were varied linearly in 32 steps. The decrease in signal was roughly about 3 orders of magnitude in order to resolve the degree of polydispersity accurately [26]. All measurements were performed at 25 °C using the PEG signal at 3.7 ppm for evaluation. The measurements were repeated 100 times for each sample to study the intra-sample variation.

3.3. Simulations

Simulated data sets were generated using both the log-normal model and the gamma model, and used to evaluate how well mean self-diffusion coefficient and spread (where applicable) were estimated using each of the four models. In

all cases, the true mean self-diffusion coefficient is $10^{-10} \text{ m}^2\text{s}^{-1}$. The k vector includes 32 different data points, distributed equidistantly in \sqrt{k} (linearly in gradient strength) between 2.5×10^7 and $2.5 \times 10^{11} \text{ m}^{-2}\text{s}^{-1}$. Using this range of k values, we ensure that the attenuation is at least 3 order of magnitude even for the broadest distributions. The true signal intensities $I(k)$ are computed for each model (from Eq. (5)). Normally distributed noise with mean zero and standard deviation $\sigma_{\text{noise}} = 0.001$ (roughly corresponding to the noise levels estimated from the experimental data sets studied in 3.2) is added to the simulated measurements. The spread is varied in the range 0%, 2.5%, 5%, ..., 47.5%, 50% (polydispersity index varying between 1 and 1.25). For every parameter setting, 1000 simulated data sets were generated to obtain reliable averages of the parameter estimates.

Simulated data sets were also generated to evaluate the computational speed for fitting of multiple component distributions. Here, the aim is not to evaluate the accuracy or precision of the estimated parameter values, but only to evaluate the fitting speed under varied, realistic conditions. Therefore, the underlying true distribution in the simulations was chosen to be a random multiple component distribution consisting of up to 3 log-normal components. In each simulation, the number of components was randomly selected as either 1, 2, or 3. The value for the mean self-diffusion coefficient for each component was randomly chosen between 0 and $5 \times 10^{-10} \text{ m}^2\text{s}^{-1}$. The value for the CV for each component was randomly chosen between 0 and 50%. For each data set, multiple component distributions with 1, 2, and 3 components, of all types, i.e. single exponential components, stretched exponential components, log-normal components, and gamma components, were fitted and the time for fitting measured. For every parameter setting, 1000 simulated data sets were generated to obtain reliable averages of the time for fitting.

3.4. Evaluation

All code was run in Matlab 7.11.0 (R2010b) using the `fmincon` optimization routine and the sequential quadratic programming (`sqp`) option for non-linear least squares fitting. Analytical derivatives were provided where possible, i.e. for the single exponential, stretched exponential, and gamma distribution models, but not for the log-normal model. Multiple fittings with different (random) initial parameter guesses were run to avoid getting stuck in locally optimal points during optimization.

The parameters of the four different models were estimated for the experimental data sets and the simulated data sets, and compared in terms of mean self-diffusion coefficient, coefficient of variation (where applicable), and polydispersity index (where applicable).

4. Results and Discussion

4.1. Experimental data sets

Normalized signal attenuations together with the corresponding model fits with residuals for PEG I and PEG II are presented in Fig. 1. The signal at-

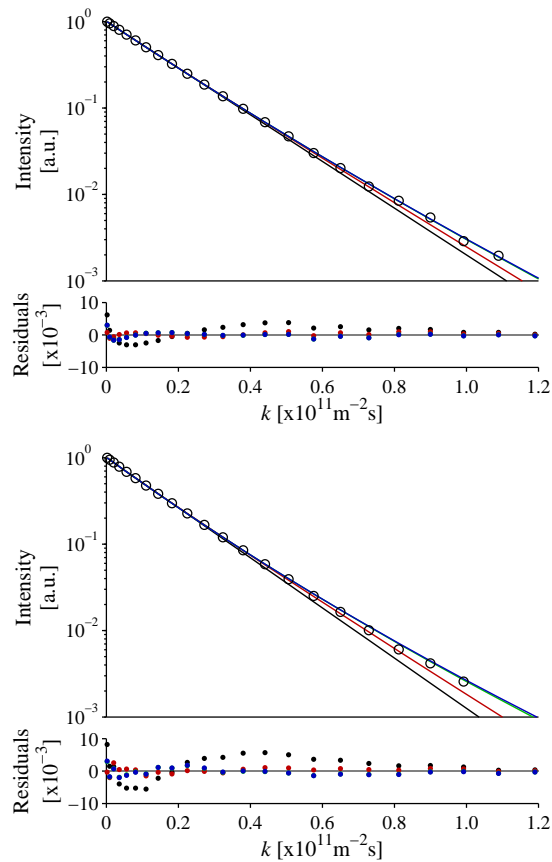


Figure 1: Example of a (normalized) experimental signal attenuation from PEG I data (top, open circles) and PEG II data (bottom, open circles) in a semi-logarithmic representation together with the fits using the single exponential (black line, residuals black filled circles), stretched exponential (red line, residuals red filled circles), log-normal distribution (green line, residuals green filled circles), and gamma distribution (blue line, residuals blue filled circles) models. Note that the log-normal and gamma models fit equally well and the residuals almost completely coincide.

tenuation for PEG II is typically characterized by a slightly more pronounced curvature at higher k -values in comparison to the attenuation for PEG I, corresponding to a higher degree of polydispersity. The residuals for all models are non-random for both PEG I and PEG II, indicating that none of them are a perfect fit. The residuals are largest and most clearly non-random for the single exponential model, which evidently provides the worst fit. The stretched exponential, the log-normal, and the gamma distribution models are comparable in terms of goodness of fit. Note in particular that for both PEG I and PEG II, the log-normal and gamma distribution models fit almost equally well and the

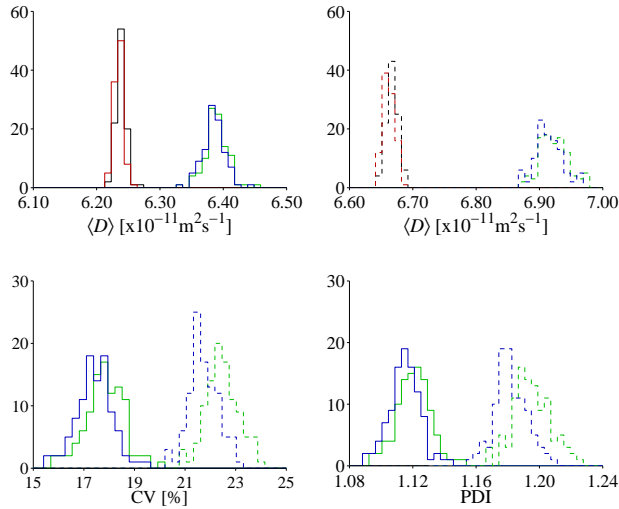


Figure 2: Histograms of estimates, based on 100 repeated experiments, of the mean self-diffusion coefficient ($\langle D \rangle$), the coefficient of variation (CV), and the polydispersity index (PDI) for the PEG I (solid line) and PEG II (dashed line) data using the single exponential (black), stretched exponential (red), log-normal distribution (green), and gamma distribution (blue) models.

residuals almost completely coincide. Histograms of the distributions of the estimated values for mean self-diffusion coefficient, CV and PDI are shown in Fig. 2. The estimated mean self-diffusion coefficients obtained for the single exponential and the stretched exponential models have very similar values. This indicates that whereas the stretched exponential provides for a better fit to the data than the single exponential, the estimate of the mean self-diffusion coefficient is no less biased. The estimated mean self-diffusion coefficients, CV, and PDI obtained for the log-normal and gamma distribution models have very similar values, also the difference that is there is slightly more pronounced for the more polydisperse PEG II. The estimated values of the mean self-diffusion coefficient and spread for the log-normal and gamma models were compared with the help of scatter plots (see Fig. 3), which further emphasize the similarity between these two models. The scatter plots indicated that the estimates are overall strongly correlated and not substantially different between the log-normal and gamma models. For all three parameters, the gamma and log-normal distribution models gave almost perfectly correlated estimates ($\rho > 0.999$ in all three cases).

4.2. Simulated data sets

We provide one simulated decay curve (for the log-normal) and the corresponding fitted models in Fig. 4. In addition, we include a comparison of the averages for the estimated values of mean self-diffusion coefficient ($\langle D \rangle$) and coefficient of variation (CV) for all models in the two cases where the true un-

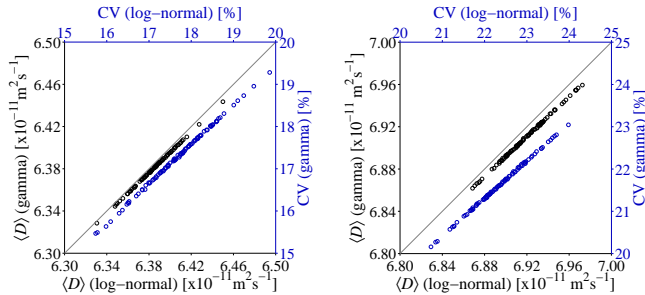


Figure 3: Scatter plots of estimates, based on 100 repeated experiments, of the mean self-diffusion coefficient ($\langle D \rangle$, black circles), the coefficient of variation (CV, blue circles) for PEG I (left) and PEG II (right) data using the log-normal distribution (horizontal) and gamma distribution (vertical) models. The gray line shows the ideal result with unit slope. The PDI behaved very similarly to the CV and was excluded here.

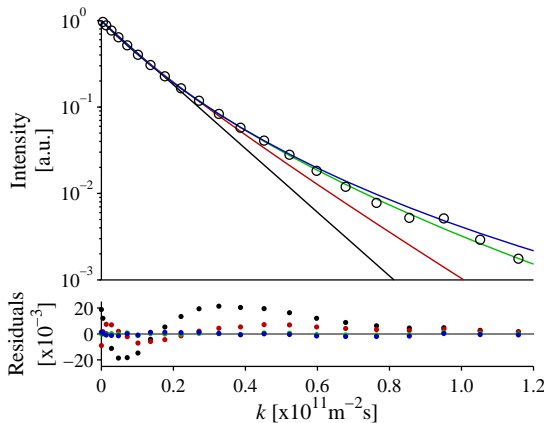


Figure 4: Example of a simulated signal attenuation curve corresponding to a log-normal distribution with 25 % spread (CV) (open circles) in a semi-logarithmic representation together with the fits using the single exponential (black line, residuals black filled circles), stretched exponential (red line, residuals red filled circles), log-normal distribution (green line, residuals green filled circles), and gamma distribution (blue line, residuals blue filled circles) models. Note that the residuals for the log-normal and gamma models almost completely coincide.

derlying distribution is either log-normal or gamma (see Fig. 5). We see that for small to moderate coefficients of variation, the four models perform comparably when estimating the mean self-diffusion coefficient. For large coefficients of variation, however, the gamma and log-normal models are superior to the single exponential and stretched exponential. Also, for very large coefficients of variation, the difference between the gamma and log-normal models is more pronounced, although the difference is not crucial.

Furthermore, we include a comparison of the computational speed for fitting of the different models (see Fig. 6). We see that the gamma model is increas-

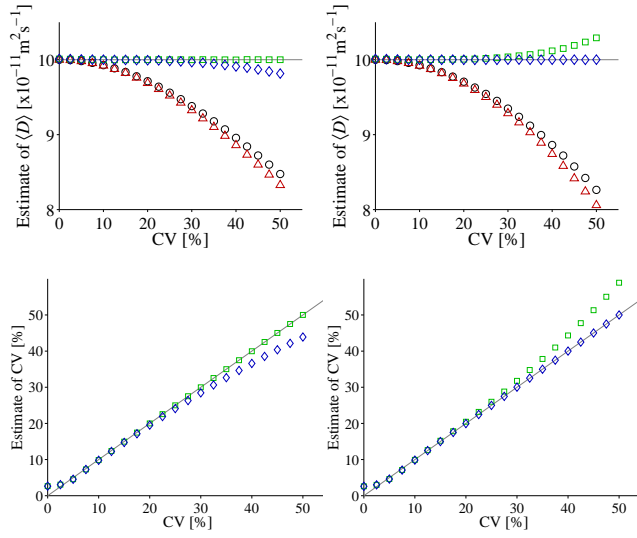


Figure 5: Average of estimated mean self-diffusion coefficients $\langle D \rangle$ and estimated coefficients of variation (CV) using the single exponential (black, circles), stretched exponential (red, triangles), log-normal distribution (green, squares), and gamma distribution (blue, diamonds) models, when the true underlying distribution is a *log-normal* (left) and *gamma* (right) with true mean self-diffusion coefficient $10^{-10} \text{ m}^2 \text{ s}^{-1}$. The mean estimates are computed from 1000 simulated attenuation curves for each value of CV. The gray line shows the ideal result.

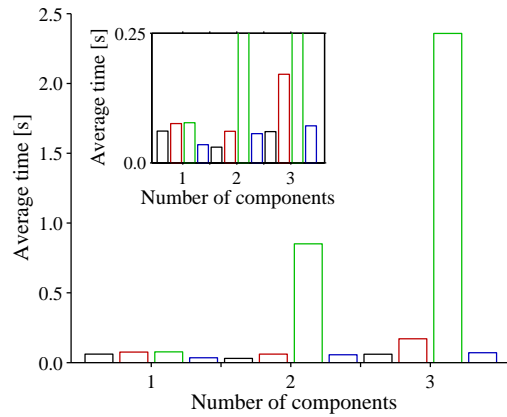


Figure 6: Average time for one fitting using the single exponential (black), stretched exponential (red), log-normal distribution (green), and gamma distribution (blue) models, each of the models with 1 (left), 2 (center), and 3 (right) components. The inset is a magnification.

ingly superior to the log-normal in terms of computational speed as the number of components increases. This is due to the number of numerical computations increasing roughly linearly in the number of components when analytical

derivatives of the objective function are supplied, but super-linearly when they are not. Surprisingly, we note that the gamma distribution is not substantially slower than the single exponential. Note that this is the computational time measured for one data fitting only. Since the number of fittings (number of random initializations) would need to be increased when the number of components increases, which we have not accounted for here, the computational time needed for fitting would actually increase much faster as a function of the number of components than this figure suggests. This makes the differences in computational speed even more pronounced. The gamma distribution is thus computationally much simpler to handle than the log-normal distribution, and should be preferable in many situations.

5. Conclusion

We conclude that the log-normal and gamma distribution models perform comparably, and that the gamma distribution model is a very competitive choice for fitting the signal attenuation in PFG NMR studies in order to estimate the distribution of self-diffusion coefficients. Except in the most extreme cases (less than 3% difference in $\langle D \rangle$ if the true CV is less than 50%), parameter estimates obtained using the gamma model were very similar to those obtained using the more widely applied log-normal model. Moreover, in terms of computational speed the gamma model is superior to the log-normal model, comparing well to the single exponential and the stretched exponential models. It is also considerably easier to implement in software compared to the lognormal. Therefore, the gamma model should be considered in many situations as an alternative to all of these three other models. In particular it should be preferable over the log-normal, especially when analyzing multi-component systems.

6. Acknowledgements

We acknowledge Peter Stilbs for careful reading of the manuscript and valuable discussions. This work is financially supported by VINNOVA through the VINN Excellence Centre SuMo Biomaterials (Supramolecular Biomaterials - Structure dynamics and properties) and the Swedish Research Council VR (grant numbers 2009-6794 and 2011-4334). The Swedish NMR Center is acknowledged for spectrometer time.

Appendix A. Derivation of the gamma distribution model

Inserting the gamma distribution,

$$P_G(D; \kappa, \theta) = D^{\kappa-1} \frac{e^{-D/\theta}}{\Gamma(\kappa)\theta^\kappa}, \quad (\text{A.1})$$

into the general expression for the NMR echo decay,

$$I(k) = I_0 \int_0^\infty P(D) e^{-kD} dD, \quad (\text{A.2})$$

we get that

$$\begin{aligned} I(k) &= I_0 \int_0^\infty P_G(D; \kappa, \theta) \exp(-kD) dD = \\ I_0 \int_0^\infty \frac{1}{\Gamma(\kappa)\theta^\kappa} D^{\kappa-1} \exp\left(-D/\left(\frac{1}{\theta} + k\right)\right) dD &= \\ I_0 \theta^{-\kappa} \left(\frac{1}{\frac{1}{\theta} + k}\right)^\kappa \int_0^\infty P_G(D; \kappa, \frac{1}{\frac{1}{\theta} + k}) dD &= \\ I_0 \theta^{-\kappa} \left(\frac{1}{\frac{1}{\theta} + k}\right)^\kappa &= \\ I_0 (1 + k\theta)^{-\kappa}. & \quad (\text{A.3}) \end{aligned}$$

Moreover, since the mean $\langle D \rangle = \kappa\theta$ and the standard deviation $\sigma_G = \sqrt{\kappa\theta^2}$, it follows that $\kappa = \langle D \rangle^2 / \sigma_G^2$ and $\theta = \sigma_G^2 / \langle D \rangle$, and the gamma distribution model can be reformulated as in Eq. (9).

Appendix B. Derivation of polydispersity index relations

The polydispersity index is defined as the ratio of the weight-average molecular weight M_w and the number-average molecular weight M_n . Assume our molecular weight M follows some (any) probability distribution, then the two quantities are defined as

$$M_w = \frac{\langle M^2 \rangle}{\langle M \rangle} \quad (\text{B.1})$$

and

$$M_n = \langle M \rangle. \quad (\text{B.2})$$

So, the polydispersity index becomes

$$\text{PDI} = \frac{M_w}{M_n} = \frac{\langle M^2 \rangle}{\langle M \rangle^2}. \quad (\text{B.3})$$

It is found in [6] that B.3 can be related to the parameters of the distribution of our self-diffusion coefficients D by the empirical relation

$$\frac{\langle M^2 \rangle}{\langle M \rangle^2} = \left(\frac{\langle D^2 \rangle}{\langle D \rangle^2} \right)^{1/\alpha^2}. \quad (\text{B.4})$$

This last step is a general formula relating PDI to the properties of the distribution of self-diffusion coefficients, which we will now compute for both the lognormal and the gamma distributions. For lognormal, we have that

$$\langle D \rangle = \exp(\mu + \sigma_L^2/2) \quad (\text{B.5})$$

and

$$\langle D^2 \rangle = \exp(2\mu + 2\sigma_L^2). \quad (\text{B.6})$$

Hence,

$$\text{PDI} = \exp\left(\frac{\sigma_L^2}{\alpha^2}\right). \quad (\text{B.7})$$

Equivalently for gamma,

$$\langle D \rangle = \kappa\theta \quad (\text{B.8})$$

and

$$\langle D^2 \rangle = \kappa(1 + \kappa)\theta^2. \quad (\text{B.9})$$

Hence,

$$\text{PDI} = \left(1 + \frac{1}{\kappa}\right)^{1/\alpha^2} = \left(1 + \frac{\sigma_G^2}{\langle D \rangle^2}\right)^{1/\alpha^2}. \quad (\text{B.10})$$

References

- [1] P. Callaghan, *Translational Dynamics and Magnetic Resonance Principles of Pulsed Gradient Spin Echo NMR*, Oxford University Press, 2011.
- [2] W. Price, *NMR studies of translational motion*, Cambridge University Press, 2009.
- [3] P. Stilbs, Fourier transform pulsed-gradient spin-echo studies of molecular diffusion, *Prog. Nucl. Magn. Reson. Spectrosc.* 19 (1987) 1–45.
- [4] P. Callaghan, D. Pinder, A pulsed field gradient NMR study of self-diffusion in a polydisperse polymer system: Dextran in water, *Macromolecules* 16 (1983) 968–973.
- [5] G. Fleischer, The effect of polydispersity on measuring polymer self-diffusion with the NMR pulsed field gradient technique, *Polymer* 26 (1985) 1677–1682.
- [6] B. Håkansson, M. Nydén, O. Söderman, The influence of polymer molecular-weight distributions on pulsed field gradient nuclear magnetic resonance self-diffusion experiments, *Colloid and Polymer Science* 278 (2000) 399–405.
- [7] H. Walderhaug, O. Söderman, D. Topgaard, Self-diffusion in polymer systems studied by magnetic field-gradient spin-echo NMR methods, *Prog. Nucl. Magn. Reson. Spectrosc.* 56 (2010) 406–425.
- [8] S. Provencher, A constrained regularization method for inverting data represented by linear algebraic or integral equations, *Computer Phys. Comm.* 27 (1982) 213–227.

- [9] S. Provencher, CONTIN: A general purpose constrained regularization program for inverting noisy linear algebraic and integral equations, *Computer Phys. Comm.* 27 (1982) 229–242.
- [10] K. Whittall, A. MacKay, Quantitative interpretation of NMR relaxation data, *J. Magn. Reson.* 84 (1989) 134–152.
- [11] I. J. Day, On the inversion of diffusion NMR data: Tikhonov regularization and optimal choice of the regularization parameter, *Journal of Magnetic Resonance* 211 (2) (2011) 178–185. doi:10.1016/j.jmr.2011.05.014.
- [12] T. Bjarnason, J. Mitchell, AnalyzeNNLS: Magnetic resonance multiexponential decay image analysis, *J. Magn. Reson.* 206 (2010) 200–204.
- [13] S. Provencher, P. Stepanek, Global analysis of dynamic light scattering autocorrelation functions, Part. Part. Syst. Charact. 13 (1996) 291–294.
- [14] B. Frisken, Revisiting the method of cumulants for the analysis of dynamic light-scattering data, *Appl. Optics* 40 (2001) 4087–4091.
- [15] J. Jensen, J. Helpert, MRI quantification of non-Gaussian water diffusion by kurtosis analysis, *NMR Biomed* 23 (2010) 698–710.
- [16] D. Topgaard, O. Söderman, Self-diffusion in two- and three-dimensional powders of anisotropic domains: An NMR study of the diffusion of water in cellulose and starch, *J. Phys. Chem. B* 106 (2002) 11887–11892.
- [17] E. Stejskal, J. Tanner, Spin diffusion measurements: Spin echoes in the presence of a time-dependent field gradient, *The journal of chemical physics* 42 (1962) 288–298.
- [18] B. Nyström, H. Walderhaug, F. Hansen, Dynamic crossover effects observed in solutions of a hydrophobically associating water-soluble polymer, *J. Phys. Chem.* 97 (1993) 7743–7752.
- [19] H. Walderhaug, B. Nyström, F. Hansen, B. Lindman, Interactions of ionic surfactants with a nonionic cellulose ether in solution and in the gel state studied by pulsed field gradient NMR, *J. Phys. Chem.* 99 (1995) 4672–4678.
- [20] X. Gong, E. W. Hansen, Q. Chen, A simple access to the (log/normal) molecular weight distribution parameters of polymers using pgste nmr, *Macromolecular Chemistry and Physics* 212 (10) (2011) 1007–1015.
- [21] P. Callaghan, D. Pinder, Influence of polydispersity on polymer self-diffusion measurements by pulsed field gradient nuclear magnetic resonance, *Macromolecules* 18 (1985) 373–379.
- [22] D. Evans, H. Wennerström, *The colloidal domain: Where physics, chemistry, biology, and technology meet*, Wiley-VCH, 1994.

- [23] J. Alper, R. Gelb, Standard errors and confidence intervals in nonlinear regression: Comparison of Monte Carlo and parametric statistics, *Journal of Physical Chemistry* 94 (1990) 4747–4751.
- [24] Y. Pawitan, *In all likelihood: Statistical modelling and inference using likelihood*, Oxford University Press, Oxford, UK, 2001.
- [25] E. Lehmann, G. Casella, *Theory of point estimation*, Springer, 1998.
- [26] B. Antalek, Using pulsed gradient spin echo NMR for chemical mixture analysis: How to obtain optimum results, *Concepts in Magnetic Resonance* 14 (2002) 225–258.